PERFORMANCE OF INTERNAL REFORMING HIGH TEMPERATURE FUEL CELLS SYSTEMS

Abdullatif B. Musa, Mosbah Talbi, and Hani Sultan

Marine Engineering Department, Faculty of Engineering,
Al-Fateh University, Tripoli, Libya
E-mail: Musa.Abdullatif@yahoo.com

الملخص

تعتبر خلايا الوقود مرتفعة درجة الحرارة (مثل خلية وقود الأكاسيد الصلبة وخلية وقود الكربونات المصهورة) مناسبة للغاية لتطبيقات توليد الطاقة الكهربائية. لقد تم معايرة وتقييم أداء نماذج خلايا الوقود المرتفعة درجة الحرارة بنوعيها، والتي تم تصميمها وإنشاءها في نموذج أسبين (Aspen customer modeller) ثم دمجت لتشكيل منظومة توليد الطاقة في(Aspen Pluse TM). في هذه الورقة تم عرض ودراسة منظومة جديدة من وحدة توليد الطاقة ذات مرحلتين؛ الأولى تتكون من كومة من خلايا وقود الأكاسيد الصلبة والأخرى من الكربونات المصهورة تشكلان معا منظومة متكاملة. في هذه المنظومة المتكاملة يتدفق الوقود بالتوازي لمصعدي الكومتين من خلايا الوقود. وزيادة على ذلك فقد تمت دراسة تأثير حقن كمية من بخار الماء في التربين الغازي على كفاءة منظومة وحدة توليد الطاقة. وبعد تقييم ومقارنة أداء منظومة خلايا وقود ألأكاسيد الصلبة والمنظومة المحقونة بالبخار والمنظومة المتكاملة، أظهرت النتائج أن كفاءة المنظومة المتكاملة مقدارها 63.5 % • بينما كفاءة المنظومة المحقونة بالبخار مقدارها 54.4 % و منظومة خلايا وقود ألأكاسيد الصلبة كفاءتها 51.8 %. أي بمعنى إن كفاءة المنظومة المتكاملة و المكونة من مرحلتين من خلايا الوقود أعلى بكثير من كفاءة وحدات توليد الطاقة ذات المرحلة الواحدة.

ABSTRACT

High temperature fuel cells such as the solid oxide fuel cell (SOFC) and the molten carbonate fuel cell (MCFC) are considered extremely suitable for electrical power plant application. Both SOFC and MCFC performances are evaluated using validated models that are built in Aspen customer modeler and integrated in Aspen Pluse ^{TM}. In this article, a new combined cycle consisting of two-staged SOFC and MCFC is proposed. In this combined cycle, the anode flows of the first and second stage fuel cell stacks are connected in parallel. Moreover, a steam injected gas turbine (STIG) cycle is considered in STIG-SOFC cycle. The performance of SOFC cycle, STIG-SOFC cycle, and combined cycle are evaluated and compared. The simulations results show that the net efficiency of the combined cycle is 63.5%. On the other hand, the net efficiency of STIG-SOFC and SOFC cycles are 54.4% and 51.8% respectively. In other words, the combined cycle with two-staged SOFC and MCFCs gives better net efficiency than the cycles with single- staged SOFC.

KAYWORDS: Fuel cells; SOFC; MCFC; Gas turbine; Performance

INTRODUCTION

Fuel cells are electrochemical devices that convert the chemical energy stored in a fuel into electrical power and have the advantage of continuous supply of reactant gases. The basic physical structure or building block of fuel cell consists of an electrolyte layer in contact with a porous anode and a cathode on either side. The main attractive features of fuel cell systems are high efficiency, quiet operation, fast load response, and near zero emissions. These being features render the fuel cells as prime candidates for providing local or national wide power systems for a sustainable economy while maintaining a clean environment. The most common classification of fuel cells is by the type of electrolyte used in the cells, and operating temperatures. Fuel cell can be divided into two types; low temperature fuel cell types and high temperature fuel cell types. The high temperature fuel cells such as solid oxide fuel cell (SOFC) and molten carbonate fuel cell (MCFC) are considered extremely suitable for electrical power plant application.

The concept of using a gas turbine (GT) or steam turbine (ST) power plant in an integrated cycle with high temperature fuel cells has been well known for many years. Waste heat recovery from turbine exhaust is known to improve GT performance significantly. In general, employing ST cycles can provide the best performance. However, a ST system requires a large bundle of equipment for ST cycles and seems to be complicated and costly [1]. The steam injected gas turbine (STIG) cycle is a gas turbine cycle in which the heat of the exhaust gas of the turbine is used to produce steam in a heat recovery steam generator [2]. This steam expanded in the gas turbine itself.

A new approach is using serially connect fuel cells. Fuel cells have a higher efficiency than gas turbines and by raising the part of the cycle power they supply, cycle efficiency can be raised. In Ref. [3], analysed a power generation system consisting of two-stages externally reformed SOFCs with serial connection of low and high temperature SOFCs. They showed that the power generation efficiency of the two-staged SOFCs is 50.3% and the total efficiency of power generation with gas turbine is 56.1% under standard operating conditions.

Hydrogen is expected to become a major energy carrier in the future energy economy. Hydrogen is not freely available in nature. As a result hydrogen is most of the time produced from fossil fuels. Hydrogen can be produced by reforming natural gas in a reformer which is fed with steam produced with waste heat available in the cycle. This is called external reforming (ER). Due to the high temperature in the high temperature fuel cells and the water production during the electrochemical reaction, SOFCs or MCFC can allow for internal reforming (IR). This means that natural gas is directly fed into the fuel cell, where it will convert to hydrogen. The heat necessary for this reforming reaction is delivered by the electrochemical reaction in the cell. The performance of internal and external reforming molten carbonate fuel cell (MCFC) systems is investigated. The simulations show that the internal reforming MCFC system is more efficient than the external reforming MCFC system [4].

In previously paper [5], Two types of combined cycles is investigated: a combined cycle consisting of a two-staged combination of IT-SOFC and HT-SOFC and another consisting of two stages of IT-SOFC. The simulation results show that a combined cycle of two-staged IT-SOFC can give 65.5% under standard operational conditions. Furthermore, by optimizing the heat recovery and the gas turbine use, the efficiency can go up to 68.3%. In other words, intermediate combined fuel cell systems

together with high temperature gas turbine systems can lead to highly efficient power cycles.

In this paper a thermodynamic models for an IR-SOFC and IR-MCFCs are developed using a process simulation tool, Aspen software. Several types of high temperature fuel cells cycles are proposed and investigated: a new combined cycle which consisting of two-staged SOFC and MCFCs and single cycle with IR-SOFC only. Moreover, in the gas turbine part, steam injected gas turbine cycle is considered in the STIG-SOFC cycle. The aim of the paper is to find the best cycle configuration.

CYCLES DESCRIPTION

The SOFC and MCFC cells currently in operation are fueled with methane. The high temperatures inside the SOFC and MCFC cells stacks can make it possible to reform the methane directly inside the cell if steam is provided at the inlet. The heat necessary for this reforming reaction is delivered by the electrochemical reaction in the cell. Water and fuel are provided at atmospheric conditions. The fuel is pure methane (CH_4). The fuel mass flow rate being burned in the combustor is varied. The characteristics of the systems are given in Table (1). Pressure is kept constant at 4 bar. The cathode inlet temperature of the SOFC stack is controlled to be 800 °C.

SOFC and MCFCs combined cycle

Figure (1) shows a cycle diagram of the combined cycle consisting of two-staged SOFC and MCFCs. Water and methane are admitted into the heat exchangers H/E2 and H/E3 to generate steam and to preheat the methane. The pre-heated methane is mixed with steam. The mixture is split into two equally parts. Part of this mixture is supplied to the anode side of the MCFC stack. The remaining part of the mixture passes to the pre-heater, where it is heated to a given temperature, and then enters into the anode side in the SOFC stack, see Figure (1). The remaining anode and cathode gases from the SOFC stack are recycled to the combustor. Part of the heat released in the combustor (stream 2) is used in the pre-heater; the remaining heat is used to heat up the burned gas. This burned gas from the combustor passes to four heat exchangers H/E1, H/E2, H/E3, and H/E4 respectively. In three of these heat exchangers the hot effluent of burned gas releases the heat necessary to preheat the cathode inlet gases, generate steam, and preheat the methane. The compressed air from the compressor (COMP2) is supplied to the heat exchanger (H/E5).The air coming from the H/E5 is further heated to 800°C at (H/E1) before it flows into the cathode side of the SOFC stack. The combustor exit gas which contains a major part of air, CO_2 and H_2O is heated at H/E4, and then is split into two parts. The first part is the cathode inlet gas of the MCFC stack. The remaining part of the combustor exit gas and cathode outlet gas of MCFC are mixed, the mixture is sent to heat exchangers (H/E6), gas turbine and heat exchangers (H/E7) and (H/E8) respectively. The remaining anode gases of the MCFC stack is recycled to the combustor.

SOFC cycles

The SOFC and STIG-SOFC cycles are presented in Figure (2) layout A and layout B. The SOFC cycles are similar to the combined cycle (Figure (1)), except that there is no MCFC stack. Therefore, in the SOFC cycle the combustor exit gas is heated at H/E4, and is sent to a gas turbine and heat exchangers (H/E7) and (H/E8) respectively. While, in the SOFC steam injected gas turbine (STIG-SOFC) cycle the

majority of steam which is generated in a heat exchanger (H/E7) is directly injected and simultaneously expanded in the gas turbine together with combustion gases, see Figure (2). There is no heat exchanger (H/E8) in STIG-SOFC cycle.

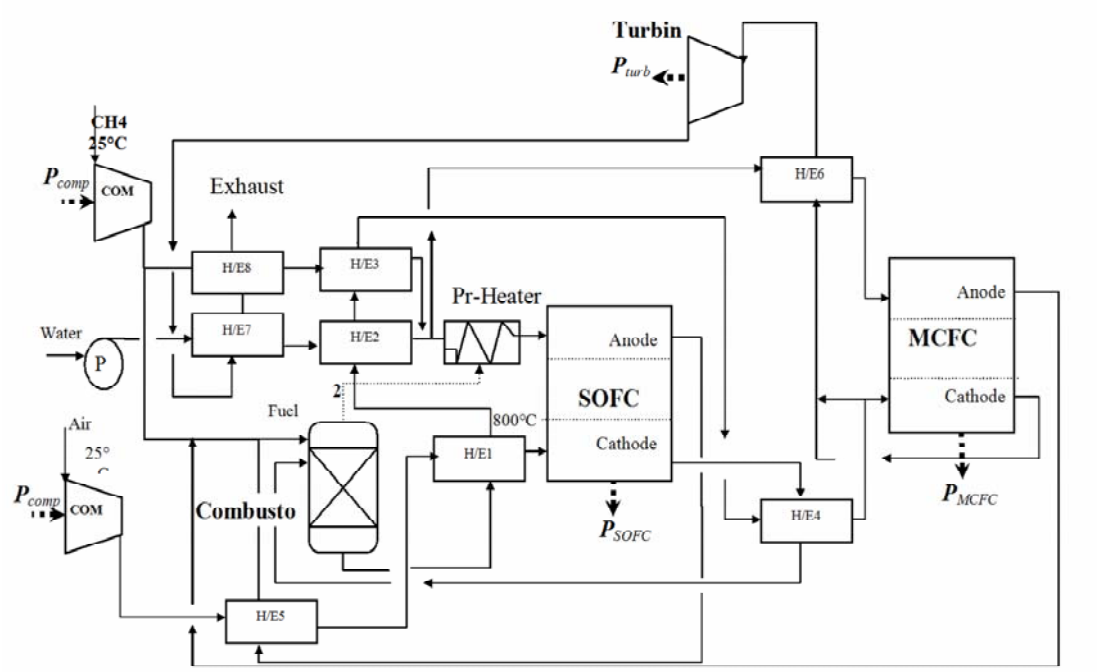

Figure 1: Schematic diagram of combined cycle (COMP: compressor; P: pump; H/E: heat exchanger)

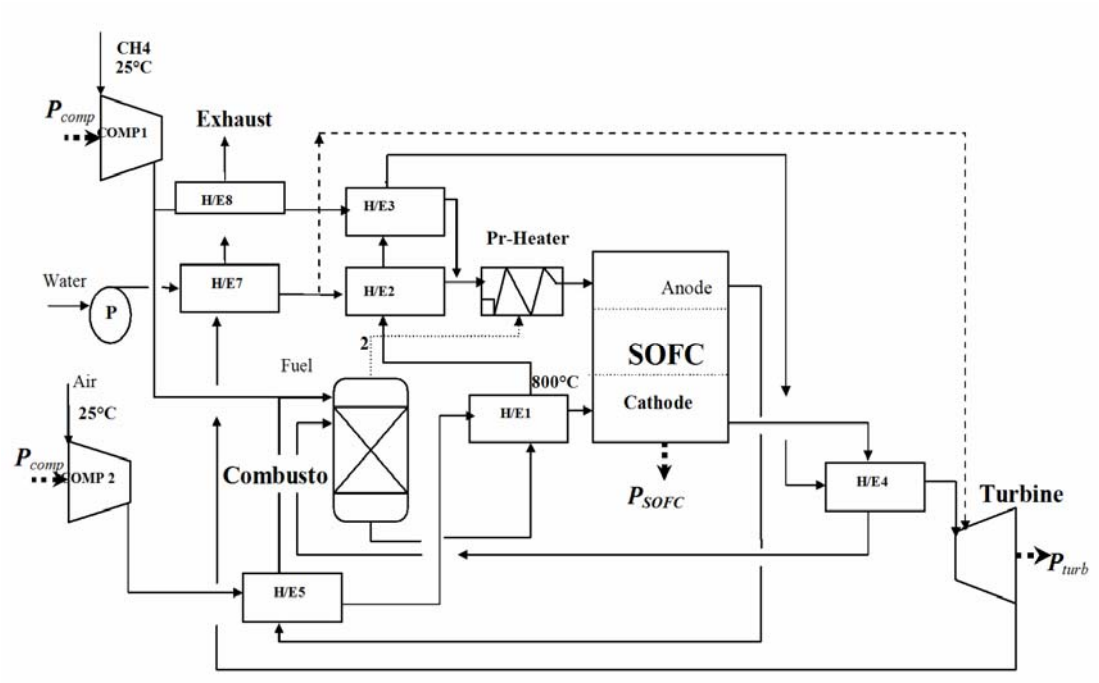

Figure 2: Schematic diagram of SOFC cycles: layout A and B (the dotted line is for B)

Table 1: Input parameters of the high fuel cells systems

Fuel cell		other devices	
S/C ratio	2	λ (air factor)combustor	1.1
P	4 bar	η for compressor	0.8
u_f *of SOFC*	85%	η for pump and turbine	0.85
u_f *of MCFC*	75%	T_{react} combustor	900°C

CYCLES ANALYSIS METHOD

Modelling assumptions

- The assumptions and conditions of the models used in the simulation program are as follows:
- steady state conditions with negligible frictional losses;
- negligible changes of potential and kinetic energies in any process;
- changes in the composition of the anode and cathode gases are only significant in the flow direction;
- oxidant and fuel are considered ideal gases;
- Nernst potential is independent of hydrostatic pressure graduations;
- the operating temperature of the cell is equal to the temperature of the outlet cathode and anode.
- pure methane (CH_4) is used as fuel.

Thermochemical aspects: water gas shift reaction and methane reforming

In the models, the chemical reactions are assumed to be in equilibrium, *i.e.* that they occur instantaneously and reach the equilibrium condition spontaneously at each position.

For SOFC models the electrochemical reactions are as follows:

$\frac{1}{2}O_2 + 2e^- \rightarrow O^{2-}$ cathode (1)

$H_2 + O^{2-} \rightarrow H_2O + 2e^-$ anode (2)

$H_2 + \frac{1}{2}O_2 \rightarrow H_2O$ overall reaction (3)

For MCFC models the electrochemical reactions are as follows:

$CO_2 + \frac{1}{2}O_2 + 2e^- \rightarrow CO_3^{2-}$ cathode (4)

$H_2 + CO_3^{2-} \rightarrow H_2O + CO_2 + 2e^-$ anode (5)

$H_2 + \frac{1}{2}O_2 \rightarrow H_2O$ overall reaction (6)

The high temperatures inside the SOFC and the MCFC stack allow for reforming the methane directly inside the cell if steam is provided at the inlet. The chemical reactions of fuel reforming and water-gas shift are as follows:

$CH_4 + H_2O \Leftrightarrow CO + 3H_2$ fuel reforming reaction (7)

$CO + H_2O \Leftrightarrow CO_2 + H_2$ water-gas shift reaction (8)

The electrochemical and water–gas shift reactions are exothermic, whereas fuel reforming is a strongly endothermic reaction.

DESCRIPTION OF THE SOFC AND MCFC MODELS

The fuel cell is treated as a single control volume in which the steady state flow energy equation is applied with the assumption of negligible change of kinetic and potential energy. In order to determine the cell performance, the overpotential must be deducted from the Nernst potential (E), which represents the ideal performance.

$$V_{cell} = E - V_{loss} \tag{9}$$

Evaluation of voltage drop in SOFC

The overpotential is expressed by activation (V_{act}), ohmic (V_{ohm}) and concentration (V_{conc}) overpotentials. Activation overpotential which estimates losses due to slow electrochemical kinetics Ohmic overpotential, which estimates losses associated with ionic and electronic resistance throughout the fuel cell. Concentration overpotential, which estimates losses due to mass transport limitations, becomes significant when amounts of current are drown from the cell [6]. The activation, ohmic and concentration overpotentials can be calculated by the following equations respectively:

$$V_{act} = ai\exp\left(\frac{b}{T}\right) \tag{10}$$

$$V_{ohm} = iR_t \tag{11}$$

$$V_{conc} = -\frac{\overline{R}T}{n_e F}\ln\left(1 - \frac{i}{i_L}\right) \tag{12}$$

The cell voltage of the SOFC can be calculated by:

$$V_{cell} = \frac{RT}{2F}\ln K + \frac{RT}{2F}\ln\left(\frac{p_{H_2} p_{O_2}^{1/2}}{p_{H_2O}}\right) - \left(V_{act} + V_{ohm} + V_{conc}\right) \tag{13}$$

Evaluation of voltage drop in MCFC

In this paper, the internal resistances of the MCFC stack can be calculated as follows the ohmic cell resistance (r_{ohm}), anodic reaction resistance ($r_{pol,an}$) and cathodic reaction resistance ($r_{pol,ca}$) are reflected in the functions of the reaction temperatures and partial pressure of gas constituents [7]. The ohmic cell resistance included the ionic and

electric resistance; it is calculated using an Arrhenius equation as function of the operating temperature as follows:

$$r_{ohm} = 0.5 \exp\left[3016 \times \left(\frac{1}{T_{cell}} - \frac{1}{923}\right)\right] \tag{14}$$

$$r_{pol,an} = 2.27 \times 10^{-5} \exp\left(\frac{6435}{T_{cell}}\right) P_{H_2}^{-0.42} P_{CO_2}^{-0.17} P_{H_2O}^{-1} \tag{15}$$

$$r_{pol,ca} = 7.505 \times 10^{-6} \exp\left(\frac{9298}{T_{cell}}\right) P_{O_2}^{-0.34} P_{CO2}^{-0.09} \tag{16}$$

The cell voltage of the MCFC can be calculated by:

$$V_{cell} = \frac{RT}{2F} \ln K - \frac{RT}{2F} \ln\left(\frac{p_{H_2O} p_{CO_2 an}}{p_{H_2} p_{CO_2 ca} \sqrt{p_{O_2}}}\right) - i \times \left(r_{ohm} + r_{pol,an} + r_{pol,ca}\right) \tag{17}$$

Electrical power of the fuel cells

The electrical power produced by the fuel cell is calculated by:

$$\dot{W} = V_{cell} I \tag{18}$$

The heat lost to the environment over the cell boundary at equilibrium can be determined by evaluating the entropy rate balance for a control volume.

$$\dot{Q}_{cv} = T\left(\Delta S - \sigma_{cv}\right) \tag{19}$$

Where:

$$\Delta S = \left(S^{\circ}_{H_2O} - S^{\circ}_{H_2} - \tfrac{1}{2} S^{\circ}_{O_2}\right) + \frac{R}{2} \ln\left(\frac{(p_{H_2})^2 p_{O_2}}{(p_{H_2O})^2}\right)$$

The entropy production, which is actually the irreversibility, is related to the electrochemical overpotential by Ref. [7]:

$$\sigma_{cv} = \frac{2F}{T} V_{loss} \tag{20}$$

Figure (3) shows a schematic diagram of thermodynamic analysis of fuel cell stack. Incoming flows into the control volume are the anode and cathode inlet gases, outgoing are the anode and cathode outlet flows. Electrical power is transported over the boundaries, and heat can also be extracted. Application of the First Law of Thermodynamics to the fuel cell stack in steady state conditions then gives the following:

$$\begin{aligned} \dot{Q} + \dot{W} &= h_{a-in}(T_{a-in})\dot{n}_{an} + h_{c-in}(T_{c-in})\dot{n}_{ca} \\ &- h_{a-out}(T_{a-out})\dot{n}_{a-out} - h_{c-out}(T_{c-out})\dot{n}_{c-out} \end{aligned} \tag{21}$$

$\dot{W}$ is the electrical power, and the indexes *a* and *c* stand for the anode and cathode gases, respectively. $\dot{Q}$ is the heat transfer rate between the fuel cell stack and the surroundings. Assuming that anode and cathode gases leave at the same temperature, T_{out} the energy balance simplifies to:

$$\dot{Q} + \dot{W} = h_{a-in}(T_{a-in})\dot{n}_{an} + h_{c-in}(T_{c-in})\dot{n}_{ca} - h_{a-out}(T_{out})\dot{n}_{a-out} - h_{c-out}(T_{out})\dot{n}_{c-out} \quad (22)$$

The operating temperature of the cell is assumed to be the outlet cathode and anode temperature. Equations (19) and (22) yield the outlet temperature T_{out} and $\dot{Q}$, where the electrical power $\dot{W}$ is given by equation (18).

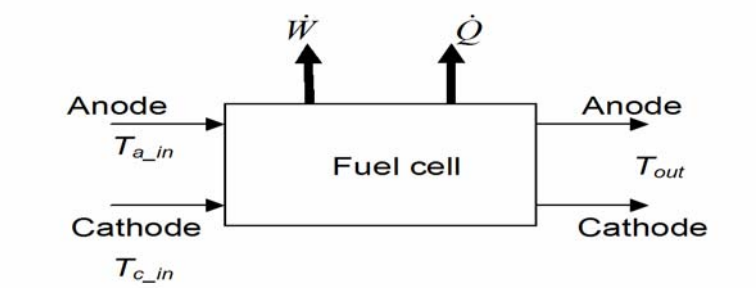

Figure 3: Schematic diagram of thermodynamic analysis of fuel cell stack

Cycle performance variables

The steam to carbon ratio is defined as the ratio between the mole flow rate of steam and the CH_4 mole flow rate to the anode.

$$S/C = \frac{\dot{n}_{H_2O}}{\dot{n}_{CH_4}} \quad (23)$$

The fuel utilisation factor is defined by:

$$u_f = \frac{\dot{n}_{H_2 consumed}}{\dot{n}_{H_2 in} + \dot{n}_{COin} + 4\dot{n}_{CH_4 in}} \quad (24)$$

The fuel cell efficiency (η_{FC}) is defined as the ratio of power produced by the fuel cell (SOFC or MCFC) to the lower heating value (LHV) of the total amount of fuel ($Q_{tot} = m_{tot} LHV$) supplied to the system.

$$\eta_{FC} = \frac{P_{FC}}{Q_{tot}} \quad (25)$$

The net cycle efficiency (η_{net}) is defined as the ratio of the power produced by the fuel cells (P_{FCs}) and the turbine, minus the total compressor power, to the (LHV) of the total amount of fuel (Q_{tot})

$$\eta_{net} = \frac{P_{FCs} + P_{turb} - P_{comp}}{Q_{tot}} \quad (26)$$

RESULTS AND DISCUSSIONS

SOFC model validation

The SOFC model has been validated against the Selimovic model and Stiller model [8-9] using the input values of a Benchmark Test (BMT). The BMT was defined by the participants of the IEA (International Energy Agency) program for the numerical simulation of SOFC planar geometry. The fuel and air flow rate were adjusted to the exact values selected by each compared model. The comparison in Table (2) shows that

the SOFC model produces similar results in the cell voltage, current density and the power. The calculated cell temperature is slightly higher in the present model. However, the difference is rather small and the model is confirmed to be a reliable tool for SOFC operation simulation. The SOFC model behaves physically correct and accurate.

Table 2: Validation of the SOFC model

	Selimovic model	Stiller model	SOFC model
Pressure (bar)	1	1	1
Fuel flow rate (mole s^{-1})	1.784×10^{-4}	1.784×10^{-4}	1.784×10^{-4}
Air flow rate (mole s^{-1})	2.901×10^{-3}	2.901×10^{-3}	2.901×10^{-3}
Inlet fuel and air temperature (K)	1173	1173	1173
Fuel utilisation (%)	85	85	85
Inlet fuel composition (molar fraction)			
H_2	0.2626	0.2626	0.2626
H_2O	0.4934	0.4934	0.4934
CH_4	0.1710	0.1710	0.1710
CO	0.0294	0.0294	0.0294
CO_2	0.0436	0.0436	0.0436
Voltage (V)	0.658	0.669	0.667
Current density (Am^{-2})	804	832	810
Power (W)	19.74	19.02	19.07
Cell temperature (°C)	1130	1063	1143

MCFC model validation

The MCFC model has been validated against the Au model using experimental results of an MCFC cell. This MCFC cell was manufactured installed and tested by Ishikawajima- Heavy Industry Co. (IHI) and was successfully operated for 3330 hours before the measurements described in Ref. [10] were performed. The anode was fed with 80% H_2 and 20% CO_2 humidified at 60°C. The cathode was fed with 70% air and 30% CO_2. Measurements were performed under atmospheric conditions. The flow rate of both anode and cathode gases were set according to the current load and required utilisation. The results of the measurements at several fuel gas flow settings are given in Table (3).

Table 3: Cell voltage as a function of current load for several fuel gas flow rates

		Cell voltage V_{cell} (mV)			
		Current density equivalent of fuel i_{in} (mA/cm^2)			
		750	375	250	188
Current density of the unit cell (mA/cm^2)	0	1056	1055	1056	1051
	30	1019	1010	1001	989
	50	993	979	966	955
	80	956	937	918	902
	100	927	909	885	868
	110	916	894	869	850
	120	901	879	852	830
	130	888	865	843	811
	140	876	848	820	794
	150	860	833	803	767
	180	801	769	729	.....

Figure (4) shows the comparison of the experimental results given by Table (3) and the simulation results of the MCFC model.

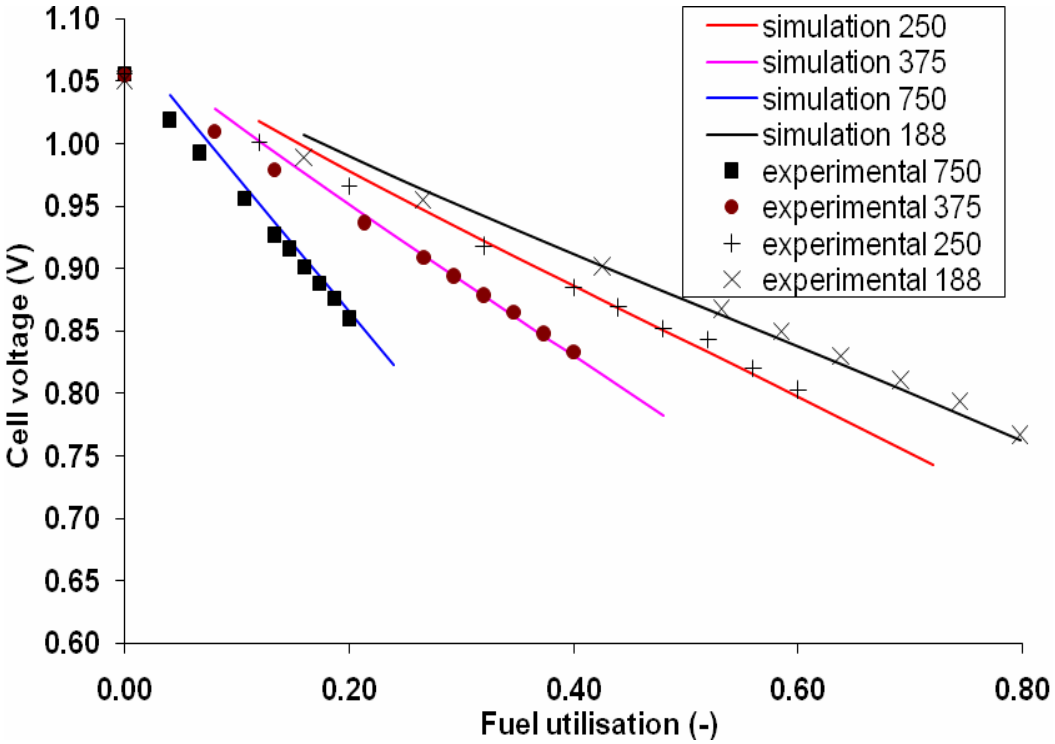

Figure 4: Comparison of the experimental results and the MCFC model

For all four different fuel gas settings, Figure (3) shows that the cell voltage decreased linearly with the fuel utilisation. For the fuel gas setting of 750, 375, and 250 mA/cm^2, the points with the highest fuel utilisation deviate slightly from linearity. These points are obtained at a current density of 180 mA/cm^2. A performance decrease at high current density is expected due to diffusion limitations, an effect not included in the model. These points are therefore omitted in the fitting. The MCFC model fits nears all the data points, except for those obtained at low fuel utilisation. Generally, a fuel cells are normally not operated at low fuel utilisation (i.e., $u_f \leq 20$). Hence, the current MCFC model is accurate.

Performance of the SOFC cycles and combined cycle

The performance of the SOFC cycle, STIG-SOFC cycle and combined cycle are evaluated and compared. The operating conditions of the SOFC stack in the cycles used in this comparison are the same. The fuel in the combustor is varied to control the temperature of anode gas inlet. In all cycles the gas temperature at the anode inlet of SOFC stack will be varied in a range between 970 and 1330°C. In this range of the gas temperature at the anode inlet the operating temperature of SOFC stack will range between 850 and 950°C in the cycles. As a result of that, the MCFC runs in the operating temperature range of around 640°C or above. The simulations of the cycles are performed at current densities 150 mA/cm.

Figure (5) shows the effect of decreasing of current density on the cell voltage of the SOFC. The load is varied by lowering the current density to 107 mA/cm². Therefore,

the fuel flow rate is lowered from 33 to 25 kg/h. The current density is an important parameter in cycle performance. When the current density is low, the amount of heat produced by the electrochemical reaction is low. Therefore, the overpotential of the SOFC decreases and causes an increase of cell voltage of the stack. The Nernst potential decreases with increase of temperature of the SOFC, and also the overpotential of the SOFC decreases with temperature. Therefore the cell voltage of SOFC reaches a maximum value as function of temperature. This maximum is shifted to higher temperatures if the current density is lower. As the operating point moves to a lower current density, the system becomes more efficient, but requires a greater fuel cell area to produce the same amount of power.

Figure (6) compares the net efficiency of the cycles. The operating temperature was changed through changing the heat input in the anode flow, by varying the fuel mass flow rate which is burned in the combustor. All net efficiency curves are relatively flat. The net efficiency of the combined cycle is bigger than of the STIG-SOFC and SOFC cycles. The total fuel consumption in the SOFC, MCFC and the combustor of the combined cycle is bigger than of single stage SOFC cycles (Figure (7)). Though the total fuel consumption is bigger in the combined cycle, the electrical output of fuel cells and gas turbine is also bigger, causing the increase in net efficiency. The net efficiency of the STIG-SOFC cycle is bigger than of the SOFC cycle, because of the recuperation of part of heat in the exhaust gas.

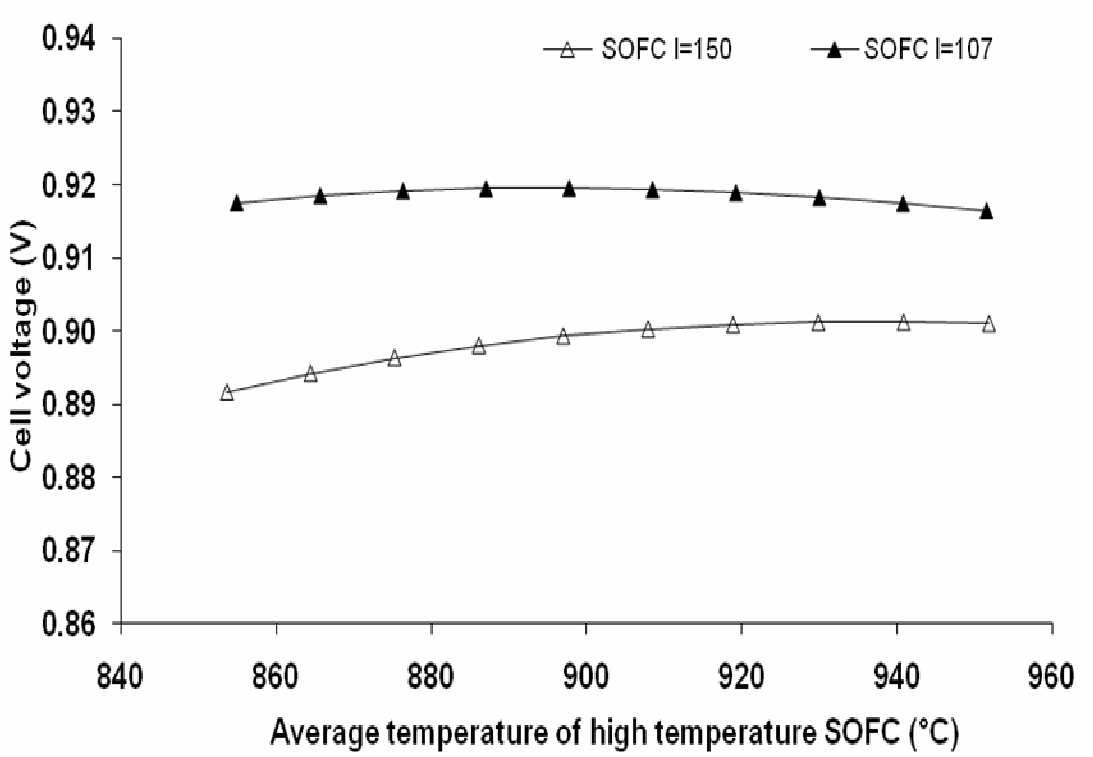

Figure 5: Effect of operating temperature on cell voltage of SOFC

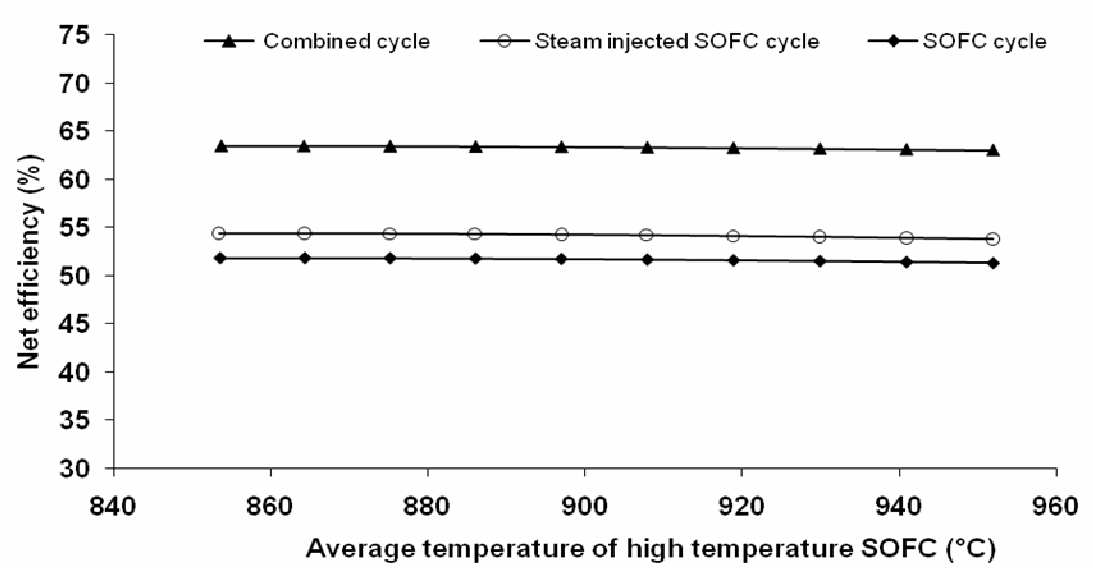

Figure 6: Net efficiency of the cycles

The gas turbine power of the STIG-SOFC cycle (Figure (8)) is bigger than of the SOFC cycle.The increase in the gas turbine power of the STIG-SOFC cycle is caused by the mass flow of steam (m_{steam} = 300 kg/h) which is injected and expanded in the gas turbine. As fuel cell can convert fuel energy more efficiently to power than the gas turbine, the output power from SOFC is bigger than the gas turbine power of the SOFC cycle. Figure (9) shows the effect of increasing the mass flow rate of steam injected to the turbine on the turbine power of SOFC-STIG cycle. As more mass flow rate of steam is injected in the gas turbine, more power can be produced resulting in an increase of the net efficiency of STIG- SOFC cycle (Figure (10)). Steam injected to a gas turbine is thus advantageous from the energy use point of view.

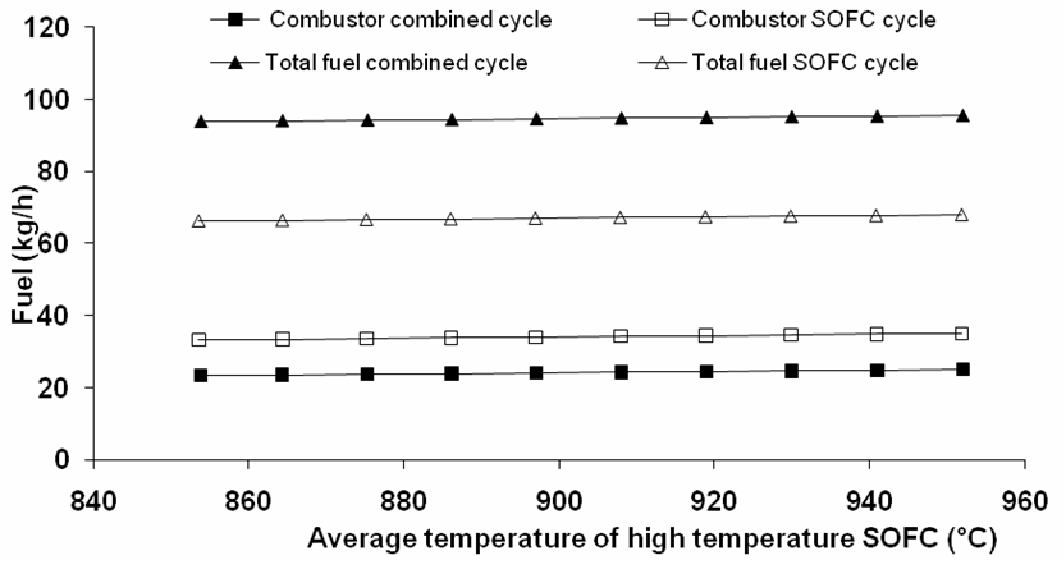

Figure 7: The fuel flow rate to the cycles

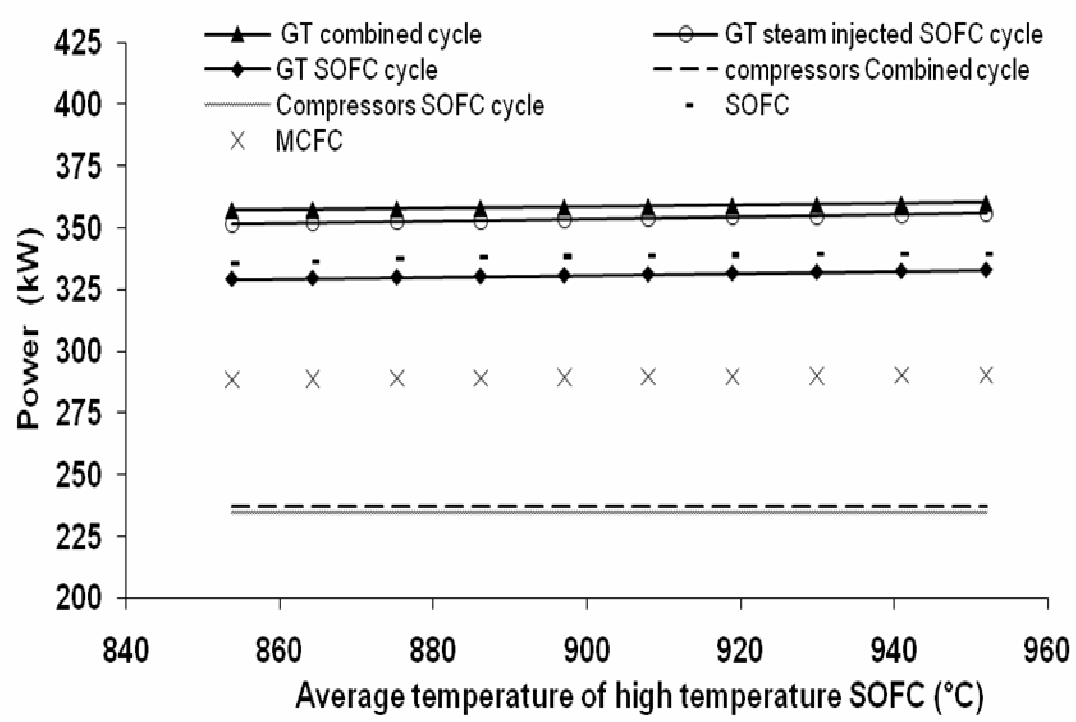

Figure 8: Fuel cells, Turbines and compressors power

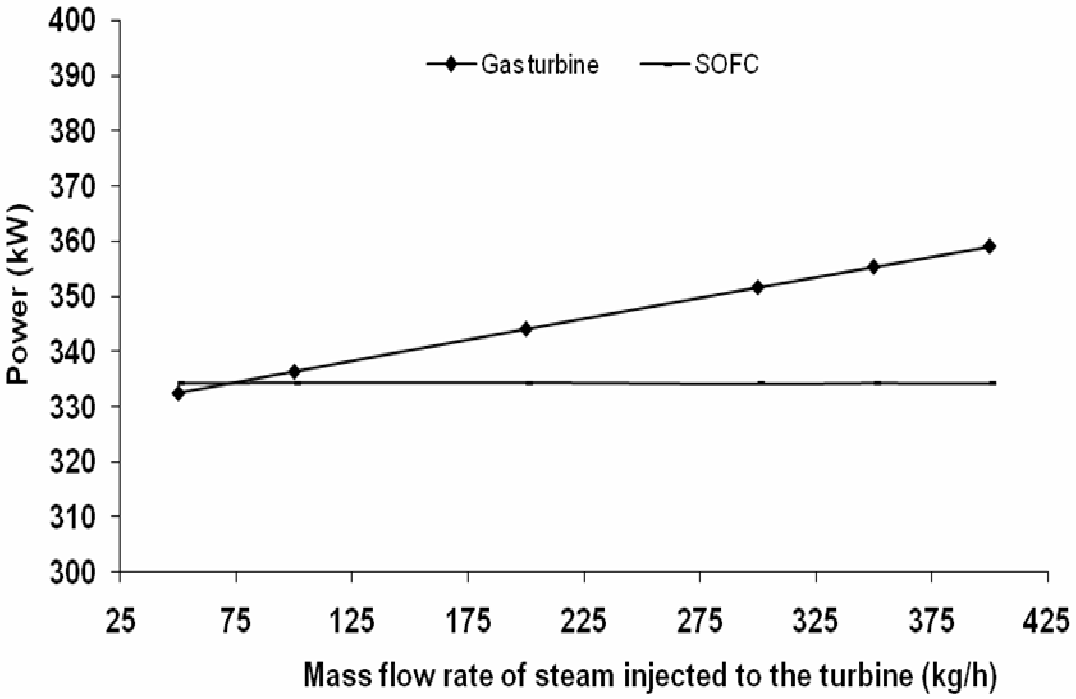

Figure 9: The effect of the mass flow rate of steam on the gas turbine power

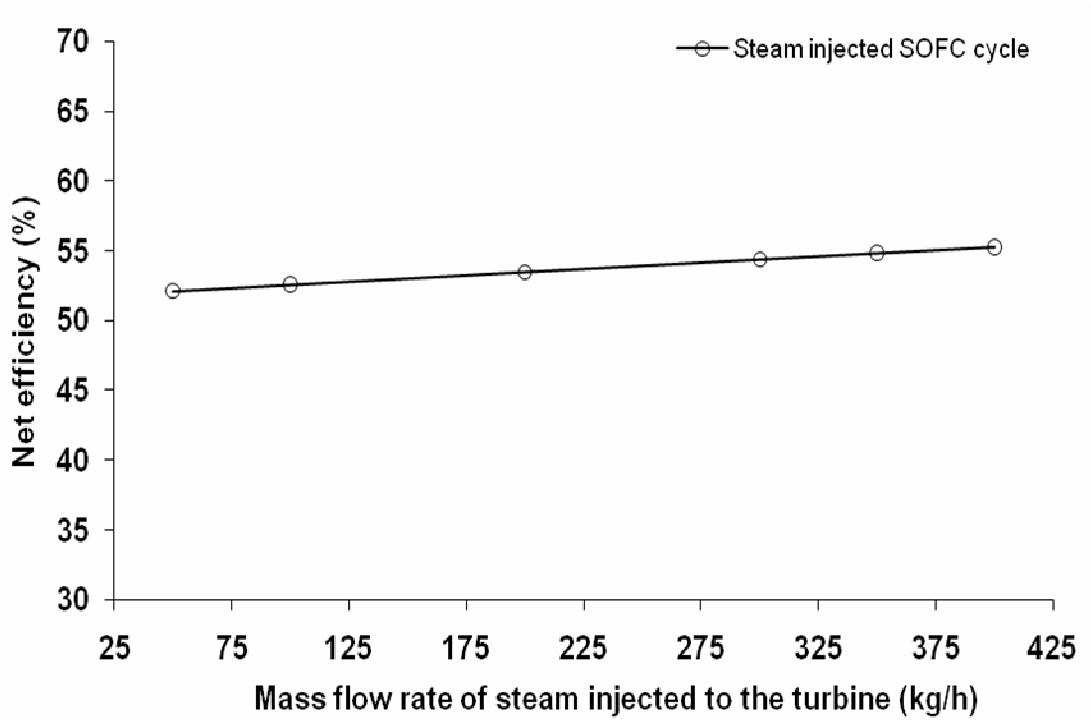

Figure 10: The effect of the mass flow rate of steam on the net efficiency

CONCLUSION

High temperature fuel cells have a great potential for developing highly efficient power cycles. They can be combined in two-staged high temperature fuel cells gas turbine cycle. Using internal reforming and a good thermal management of the cycle can result in very high cycle efficiency.

In this paper, a new combined cycle which consisting of two-staged SOFC and MCFC is proposed. The performance of SOFC cycle, STIG-SOFC cycle and combined cycle are evaluated and compared.

The simulations results show that as more mass flow rate of steam is injected in the gas turbine; more power can be produced resulting in an increase of the net efficiency of STIG-SOFC cycle. The net efficiency of the combined cycle is 63.5%. On the other hand, the net efficiency of STIG-SOFC and SOFC cycles are 54.4% and 51.8% respectively. In other words, the combined cycle with two-staged SOFC and MCFCs gives better net efficiency than the cycles with single- staged SOFC.

ACKNOWLEDGMENT

The authors acknowledge National Authority for Scientific Research and AL-Fateh University, Tripoli, Libya for the support of this work

REFERENCES

[1] Kuchonthara, P., Bhattacharya, S, Tsustsumi, A., "Combination of solid oxide fuel cell and several enhanced gas turbine cycles", Journal of Power Sources 124(2003), 65-75

[2] De Paepe, M., Dick, E., "Cycle improvements to steam injected gas turbines", Journal of Energy Research 24(2000), 1081-1107.

[3] Araki, T., Ohba, T., Takezawa, S., Onda, K., Sakaki, Y., "Cycle analysis of planer SOFC power generation with serial connection of low and high temperature SOFCs", Journal of Power Sources 158(2006), 52-59.
[4] Musa, A., Steeman, H.J., De Paepe, M., "Performance of internal and external reforming molten carbonate fuel cell systems", ASME Journal of Fuel Call Science and Technology, 4 (2007), 65-71.
[5] Musa, A., De Paepe, M., "Performance of combined internally reformed intermediate/high temperature SOFC cycle compared to internally reformed two-staged intermediate temperature SOFC cycle", International Journal of Hydrogen Energy, 33 (2008), 4665-4672.
[6] Kimijima, S., kasagi, N., "Cycle analysis of micro gas turbine-molten carbonate fuel cell hybrid system", International Journal of JSME 48(2005), 65-74.
[7] Chan, S.H., Low, C.F, Ding, O.L., "Energy and exergy of simple solid-oxide fuel-cell power systems", Journal of Power Sources 103(2002), 188-200.
[8] Selimovic, A., "Modelling of SOFC Applied to the Analysis of Integrated Systems with Gas turbines", Doctoral Thesis, Lund Institute of Technology, Sweden,2002
[9] Stiller, C., "Design, Operation and Control Modelling of SOFC/GT Hybrid Systems", Doctoral Thesis, Norwegian University of Science and Technology, Norway, 2006.
[10] Au, B., McPhail, S., Woudstra, N., K.Hemmes, "The influence of operating temperature on the efficiency of a combined heat and power fuel cell plant", Journal of Power Sources 122(2003), 37-46.

Nomenclature

A_{cell}	active cell area (m²)
E	Nernst potential (V)
F	faraday's constant (96487 kC kmol^{-1})
h	specific enthalpy (kJ kmol^{-1})
i	current density (A cm^{-2})
i_L	limiting current density (A cm^{-2})
p	partial pressure (Pa)
n	molar flow (mol s^{-1})
P_{FCs}	fuel cell stacks electrical power (kW)
P_{Comp}	compressor Power (kW)
P_{turb}	turbine power (kW)
$\dot{Q}_{cv}$	heat transfer rate in a control volume (kW)
$\dot{Q}$	heat (kW)
R_t	ohmic resistance of HT-SOFC material (Ω m²)
$\overline{R}$	universal gas constant (8.314 kJ kmol^{-1}K^{-1})
R_{tot}	cell resistance of IT-SOFC satck (Ω cm^{-2})
S/C	steam-to-carbon ratio
s	specific entropy (kJ kmol^{-1}K^{-1})
T_{cell}	cell temperature (°C)
u_f	total fuel utilization
V_{cell}	cell voltage (V)
V_{act}	activation overpotential (V)
V_{ohm}	ohmic overpotential (V)

V_{conc} concentration overpotential (V)

$\dot{W}_{cv}$ work transfer rate in a control volume (kW)

Greek letters

η efficiency (%)

$\dot{\sigma}_{cv}$ entropy production in a control volume (kW K^{-1})

Subscripts and Superscripts

0 at standard temperature and pressure

i initial

p product

R reaction or reactants